

# Physical aspects of changes in light-emitting structures with InGaN/GaN quantum wells during heating and short-term electrical influences

© A.M. Ivanov, A.V. Klochkov

Ioffe Institute, St. Petersburg, Russia

e-mail: alexandr.ivanov@mail.ioffe.ru

Received November 02, 2024

Revised February 12, 2025

Accepted February 24, 2025

The possibility of improving optical characteristics at the initial stages of aging of nitride quantum-dimensional structures by heating to a temperature not exceeding 84°C has been experimentally confirmed. The constructed chamber made it possible to carry out temperature measurements of relative changes in the external quantum efficiency and spectral density of low-frequency noise when heated to 100°C. The observed improvements in external quantum efficiency and optical power of UV LEDs occur under milder thermal conditions than in blue LEDs. Explanations of the obtained results are based on changes in the tunnel transport of carriers into quantum wells and the interaction of defects arising in them with indium.

**Keywords:** external quantum efficiency, hopping tunnel conductivity, low-frequency noise.

DOI: 10.61011/EOS.2025.04.61414.7296-24

The design of solid-state light sources, which are intended for mass production, generates increased interest in the study of aging processes in optoelectronic devices and structures based on gallium nitride, their reliability, degradation rate, and estimates of failure-free operation time. LED structures with quantum wells (QWs) based on nitride materials are also widely used in InGaN/GaN and AlGaIn/GaN LEDs and lasers in industrial and agricultural production, biology, and medicine.

The determination of mechanisms of carrier transport and degradation of light-emitting characteristics of optoelectronic devices is important for design work and refinement of the process of fabrication of LEDs and lasers based on nitride materials. One of the experimental research directions is the study of physical processes in light-emitting structures under heating (including the process of heating by an electric current flowing through them). It was reported that the luminescence intensity and external quantum efficiency (EQE)  $\eta$  decrease at above-room temperatures [1–3].

The measurement of low-frequency noise density is one of the methods for non-destructive examination of processes in semiconductor devices [4]. Excess noise levels may be used to predict the degradation rate of microelectronic components, such as lasers and LEDs [5]. The physical nature, power, and spectral composition of noise in light-emitting devices are largely determined by the spectrum of defects: their positioning in the band gap, recharging, and changes in their composition. Their emergence is attributable to the influence of hot carriers on the semiconductor lattice atoms in the process of current flow [6,7] and to an energy similar in magnitude to the material band gap released in the crystal in recombination processes [8].

The aim of the present study was to demonstrate experimentally the possibility of improving the initial pa-

rameters of optoelectronic devices made of gallium nitride. Comparative studies were performed for LEDs heated to 84°C and heated by currents to 190 mA under forward bias for the purpose of establishing the potential for initial enhancement of their characteristics under elevated temperatures, which should help slow down the degradation of device parameters.

Industrial ultraviolet LEDs with InGaIn/GaN QWs, emission wavelength  $\lambda = 375$  nm (peak emission energy  $h\nu_{\text{QW}} = 3.31$  eV), and an EQE of 30% (Nichia NSPU510CS, „T1 3/4“ [9] package) were used in the experiment. The approximate active area of these LEDs was  $10^{-3}$  cm<sup>2</sup>, and the rated operating current was  $I = 20$  mA. Temperature measurements were performed in a chamber that allows testing LEDs in a single cycle from room temperature to 100°C. Only the relative magnitude of photocurrent (optical power) and EQE changes were determined using an FD-7K silicon photodiode under short-circuit conditions.

The table presents an approximate estimate of LED overheating by current under forward bias. These calculations and measurements of the spectral density of low-frequency noise have already been reported in [10,11].

Figure 1 shows the results of examination of changes in the characteristics of UV LEDs in three consecutive exposures to currents exceeding the nominal value. Figure 1, *a* reveals a sharp increase in EQE with an increase in current at  $I < 0.1$  mA, which transitions to a section with virtually no dependence of efficiency on current at  $I > 1$ . The main finding is that the EQE value increases by  $\sim 20\%$  after 1 h of exposure to a current of 80 mA. The reduction in efficiency after exposure to 150 mA (1 h) is seen in the  $I < 0.07$  mA region. The inset in Fig. 1, *a* illustrates the changes in threshold voltage  $V_{\text{th}}$ .

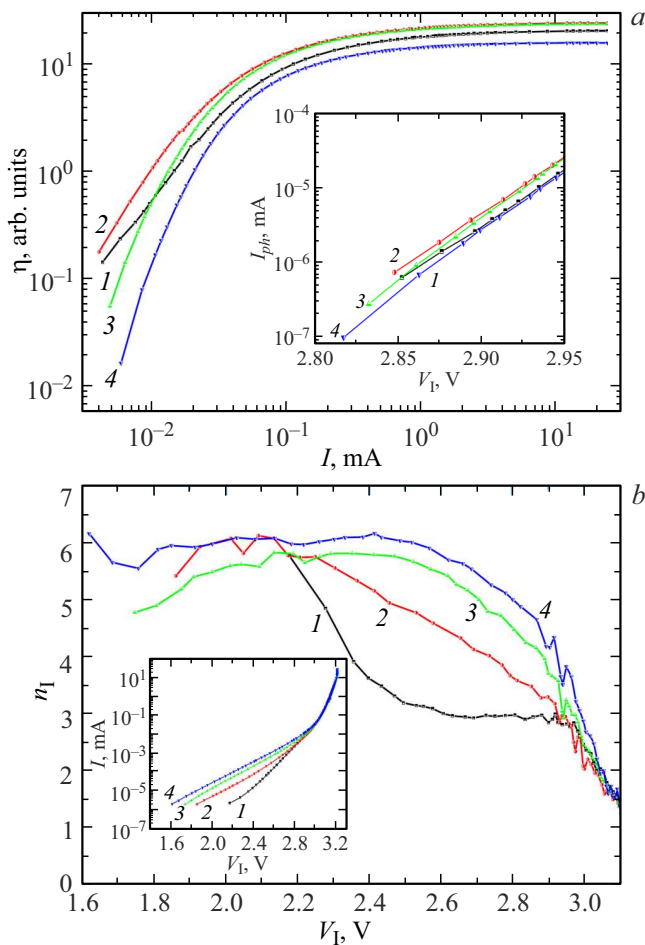


**Figure 1.** (a) Current dependences of EQE of a UV LED under forward bias: (1) before and (2–4) after three consecutive exposures to current flow (time, 1 h;  $I$ , mA: 2 — 80, 3 — 150, and 4 — 190). Dependences of the photodiode photocurrent on the  $p$ – $n$  junction voltage of the LED under study are shown in the inset. (b) Calculated dependences of the ideality factor on the  $p$ – $n$  junction voltage. Dependences of the current strength on the  $p$ – $n$  junction voltage of the LED under study are shown in the inset. The numeric designations are the same.

Current heating of UV LEDs under forward bias

Current $I$ , mA	Power $W$ , W	Overheating $\Delta T$ , °C
80	0.285	40
150	0.445	85
190	0.739	110

The calculation of dependences of the ideality factor helps reveal the nature of current flowing in LEDs. The dependences of current on the  $p$ – $n$  junction voltage,  $I(V_1)$ ,  $V_1 = V - Ir_s$ , were calculated in order to determine ideality factor  $n_1(I)$ . A series resistance  $r_s$  value of  $\sim 5 \Omega$  was determined from the linear section of dependence  $V(I)$ . Approximating the  $I(V_1)$  current–voltage curves (inset in Fig. 1, b) with function  $\exp(qV_1/n_1(V_1)kT)$ , where  $kT$  is

the thermal energy and  $q$  is the electron charge, one may calculate the dependence of the ideality factor on the  $p$ – $n$  junction voltage,

$$n_1(V_1) = (q/kT)/(d \ln I/dV_1)$$

(Fig. 1, b). Since  $n_1(V_1) \geq 2$  at bias  $V_1 < 3$  V, the current associated with tunneling through defects and tails of the density of states of allowed bands plays a significant part within this voltage range. Since  $n_1(V_1)$  increases within the  $2.2 \text{ V} < V_1 < 3 \text{ V}$  interval after each successive exposure to current, eventually reaching  $n_1(V_1) = 6$ , the fraction of carriers undergoing a subbarrier transition through the space charge regions (SCRs) and reaching QWs via hopping conduction also increases. This is facilitated by the process of alteration of the spectrum of defects: the emergence of centers (possibly metastable) providing tunnel transport of carriers to QWs. At  $V_1 \geq 3$  V, most carriers are transported into QWs by the mechanism of over-barrier injection. In this case, the series resistance in the  $p$ – $n$  junction circuit, which slowed down the growth of current, cannot be regarded as a fixed-value resistor [6].

The formation of defects involved in nonradiative recombination is currently believed to be the main mechanism of degradation of InGaN and AlGaIn LEDs. Figure 1, a proves that degradation may proceed non-monotonically. The EQE of LEDs increased after exposure to a current of 80 mA (1 h). The most general approach to the analysis of variation of emission intensity is the use of the ABC model, which represents the competition of radiative and nonradiative recombination processes. According to this model, the internal quantum efficiency is

$$\eta_{\text{int}} = Bn^2/[An + Bn^2 + Cn^3 + F(n)],$$

where  $A$ ,  $B$ , and  $C$  are the coefficients of nonradiative Shockley–Read–Hall recombination and radiative and non-radiative Auger recombination, respectively, and term  $F(n)$  characterizes the delocalization of carriers in QWs ( $n$  is their concentration) and their probable leakage [12]. These phenomena are characterized by electron delocalization current

$$I_{\text{ed}} = k(n - n_0)^s$$

and leakage current [13]

$$I_{\text{leak}} = \alpha I^p.$$

The increase in EQE after exposure to a current of 80 mA (1 h) is most significant at  $I < 100 \mu\text{A}$ . Tunneling to QWs plays an important role within this section of the current dependence. The tunnel transport of carriers to QWs reduces the value of  $F(n)$ , accelerating localization of carriers and reducing their leakage from QWs, which is beneficial for the threshold current (inset in Fig. 1, a). Following subsequent exposure to currents of 150 and 190 mA (1 h), the EQE starts decreasing: coefficient  $A$  is related to the degree of perfection of the InGaIn/GaN structure, since it is proportional to the defect density,

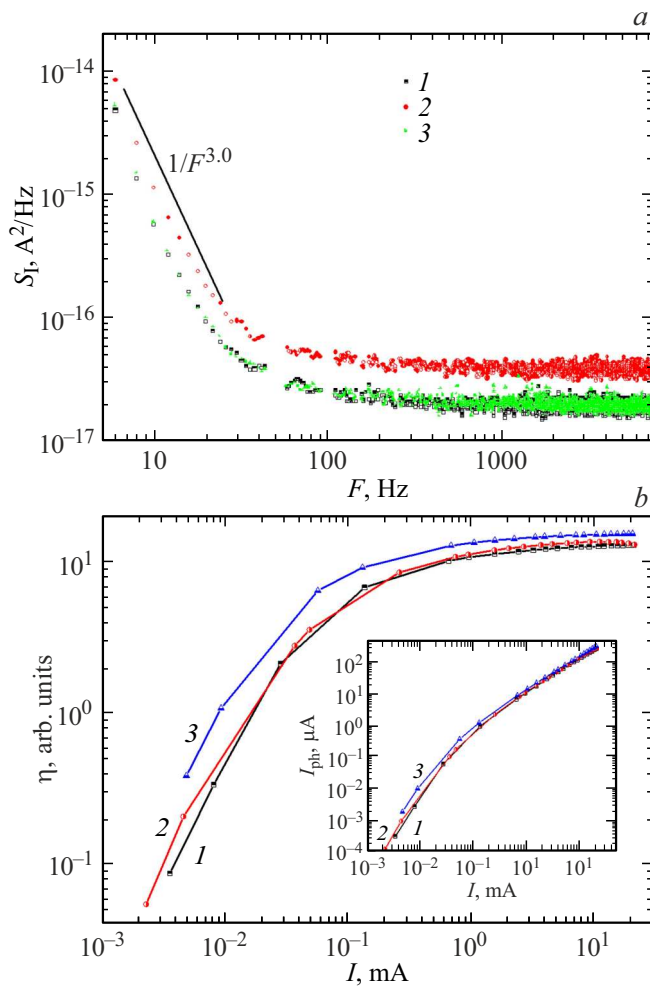


**Figure 2.** (a) Dependences of the spectral density of current noise for a UV LED at  $T, ^\circ\text{C}$ : 1, 3 — 23; 2 — 84. 3 — after 2.5 h of annealing at  $84^\circ\text{C}$ . (b) Current dependences of EQE under forward bias. The inset shows the dependences of the photodiode photocurrent on current under forward bias. The numeric designations are the same.

thermal velocity, and carrier capture cross section. Defect formation enhances nonradiative recombination. Following exposure to a current of 190 mA (1 h), the EQE decreases by a factor of 1.5 at  $\sim 20$  mA. An increase in concentration of carriers in a QWs hinders their localization, and their distribution over the QWs becomes less uniform, causing polarization [12]. Nonradiative recombination is also facilitated by the redistribution of carriers in the course of current filamentation (current crowding) [14,15].

Figure 2, *a* shows the dependences of the low-frequency noise density at nominal currents for temperatures of 23 (before and after the test with annealing in air at a temperature of  $84^\circ\text{C}$  for 2.5 h and a day of LED storage in air at room temperature) and  $84^\circ\text{C}$ . With increasing temperature, the noise density increased by  $\sim 80\%$  at  $84^\circ\text{C}$ . After the exposure, the dependence of current noise on frequency at room temperature matches the original

dependence almost perfectly. This indicates that the defects resulting from this exposure are metastable (reversible) in nature or do not affect the noise. According to Hooge's formula, the spectral density of  $1/F$  current noise is

$$S_I = (\alpha I^2)/(FN),$$

where  $\alpha$  is the Hooge constant and  $N$  is the number of electrons involved in conduction. The observed noise is associated with changes in carrier density ( $N$ ) due to generation-recombination and tunneling into and out of QWs. The density of low-frequency noise increases markedly at frequency  $F < 100$  Hz:  $S_I \sim 1/F^3$ , which suggests that the contributions of several possible noise formation mechanisms are summed up: flicker noise is combined with telegraph noise, generation-recombination noise, and noise of tunnel resistance that is determined by the non-uniformity of its distribution over the space charge region of the barrier and non-uniform filling of the centers (levels in the band gap, BG) of tunneling [16].

An increase in EQE relative to the efficiency at room temperature (experiment presented in Fig. 2) was observed when the LED was heated to  $84^\circ\text{C}$  at  $I < 10 \mu\text{A}$  and at  $I > 1$  mA (Fig. 2, *b*). This contradicts the lowering of coefficient  $B$  [17] and the reduction in efficiency of InGaN/GaN LEDs under heating. One possible explanation is the enhancement of hopping conduction [18] and tunnel carrier current in barriers [2]. Measurements performed after heating and holding at room temperature for 24 h revealed an increase in efficiency compared to the initial value within the entire current measurement range and an increase in radiation intensity (inset in Fig. 2, *b*) (by  $\sim 20\%$  and  $\sim 18\%$ , respectively, at nominal current). In the case of heating with a current of 80 mA, the same EQE enhancement is achieved at a lower temperature (see the table).

The consequences of defect formation in QWs are closely related to the state of indium in them: its concentration, distribution specifics, and clustering [19].

At the initial stages, UV LEDs degrade faster than blue ones [20,21], since indium clustering increases the localization potential and luminescence [22]. The obtained results confirm that changes in the optical characteristics of UV LEDs are initiated at weaker temperature influences than those required for blue LEDs. A higher In concentration translates into deeper carrier localization in blue LEDs, and an increase in temperature enlarges the fraction of non-localized carriers [3]. Optimization of the composition of the solid solution in a QWs becomes paramount [1], since the emerging defects are localized at heteroboundaries and composition fluctuations [23].

The improvement of certain LED parameters (Figs. 1, 2) is associated with changes in the state of indium in QWs. During operation, point defects are produced at a higher rate in regions with a lower indium content [6]. When a QWs is heated, In gets redistributed through recombination-stimulated diffusion [23], which contributes

to an improvement of conditions for carrier localization over the entire QWs width.  $I_{ed}$ ,  $I_{leak}$ , and the carrier lifetime with respect to radiative recombination decrease. This explains the observed EQE increase at the initial stages of aging.

Changes in the transport of carriers contribute to the increase in EQE under minor thermal influences. The production or rearrangement of point defects in the BG of GaN does not only intensify nonradiative recombination (raise the value of coefficient  $A$  of the model), but also enhances the tunnel component of conduction via deep levels and tails of the density of states in the BG. The enhancement of tunnel (hopping) conduction in barriers to a QWs due to a change in the spectrum of defects provides an explanation both for the EQE increase and for the suppression of noise associated with the tunnel resistance. This inhibits the overall growth of the spectral density of low-frequency noise, neutralizing the increase in, e.g., the density of generation-recombination noise.

Comparative studies have verified the potential for improvement of the initial parameters of UV LEDs through the use of thermal influences weaker than those required for blue LEDs. The concentration of indium and its state in QWs play a significant part in this. The main mechanism of aging is defect formation in QWs and adjacent barriers. Indium, which contributes to radiative recombination, helps prevent the formation of defects under electrical stress and inhibits the manifestation of emerging defects in nonradiative recombination, since it facilitates carrier localization with subsequent radiative recombination. This explains the EQE increase after heating by a current of 80 mA (1 h) and annealing at 84°C (2.5 h). Weak influences of this kind have a positive effect on the migration of point defects and the redistribution of indium in QWs. A more uniform distribution of indium in a QWs helps slow down the process of defect formation and enhance radiative recombination.

The second factor of growth of optical power and EQE at the initial stages of aging is the potential to improve carrier transport in QWs. Defects forming in barriers contribute to nonradiative recombination, but also facilitate carrier tunneling to QWs. These opportunities for improving the optoelectronic characteristics of devices should be taken into account when one adjusts the device morphology.

## Conflict of interest

The authors declare that they have no conflict of interest.

## References

- [1] M-J. Lai, Y-T. Chang, S-C. Wang, S-F. Huang, R-S. Liu, X. Zhang, L-C. Chen, R-M. Lin. *Molecules*, **27**, 7596 (2022). DOI: 10.3390/molecules27217596
- [2] N.M. Shmidt, E.I. Shabunina, A.E. Chernyakov, A.E. Ivanov, N.A. Tal'nishnikh, A.L. Zakgeim. *Tech. Phys. Lett.*, **46** (12), 1253 (2020). DOI: 10.1134/S1063785020120275.
- [3] D.S. Sizov, V.S. Sizov, E.E. Zavarin, V.V. Lundin, A.V. Fomin, A.F. Tsatsul'nikov, N.N. Ledentsov. *Semiconductors*, **39** (4), 467 (2005).
- [4] B.I. Yakubovich. *Nadezhnost'*, **17** (2), 31 (2017). DOI: 10.21683/1729-2646-2017-17-2-31-35
- [5] B. Šaulys, J. Matukas, V. Palenskis, S. Pralgauskaitė, G. Kulikauskas. *Acta Phys. Pol. A*, **119** (4), 514 (2011). DOI: 10.12693/APhysPolA.119.514
- [6] F.I. Manyakhin. *Semiconductors*, **52** (3), 359 (2018). DOI: 10.1134/S1063782618030168.
- [7] J. Ruschel, J. Glaab, B. Beidoun, N.L. Ploch, J. Rass, T. Kolbe, A. Knauer, M. Weyers, S. Einfeldt, M. Kneissl. *Photonics Res.*, **7** (7), B36 (2019). DOI: 10.1364/PRJ.7.000B36
- [8] N. Renso, C. De Santi, A. Caria, F. Dalla Torre, L. Zecchin, G. Meneghesso, E. Zanoni, M. Meneghini. *J. Appl. Phys.*, **127**, 185701 (2020). DOI: 10.1063/1.5135633
- [9] Nichia Corporation Specifications for UV LED NSPU510CS. [Electronic source]. URL: [https://led-ld.nichia.co.jp/en/product/led\\_product\\_data.html?type=NSPU510CS+%28375nm%29&kbn=1](https://led-ld.nichia.co.jp/en/product/led_product_data.html?type=NSPU510CS+%28375nm%29&kbn=1)
- [10] A.M. Ivanov. *Tech. Phys.*, **66** (1), 71 (2021). DOI: 10.1134/S1063784221010114.
- [11] A.M. Ivanov, G.V. Nenashev, A.N. Aleshin. *J. Mater. Sci.: Mater. Electron.*, **33**, 21666 (2022). DOI: 10.1007/s10854-022-08955-7
- [12] Q. Lv, J. Gao, X. Tao, J. Zhang, C. Mo, X. Wang, C. Zheng, J. Liu. *J. Lumin.*, **222**, 117186 (2020). DOI: 10.1016/j.jlumin.2020.117186
- [13] P. Sahare, B.K. Sahoo. *AIP Conf. Proc.*, **2220**, 040008 (2020). DOI: 10.1063/5.0001262
- [14] M. Shatalov, G. Simin, V. Adivarahan, A. Chitnis, S. WU, R. Pachipulusu, V. Mandavilli, K. Simin, J.P. Zhang, J.W. Yang, M.A. Khan. *Jpn. J. Appl. Phys.*, **41** (8), 5083 (2002).
- [15] A.E. Chernyakov, M.E. Levinshtein, N.A. Tal'nishnikh, E.I. Shabunina, N.M. Shmidt. *J. Cryst. Growth.*, **401**, 302 (2014). DOI: 10.1016/j.jcrysgro.2013.11.097
- [16] N.I. Bochkareva, Y.G. Shreter. *Phys. Solid State*, **64** (3), 371 (2022). DOI: 10.61011/EOS.2025.04.61414.7296-24.
- [17] P. Tian, J.J.D. McKendry, J. Herrnsdorf, S. Watson, R. Ferreira I.M. Watson, E. Gu, A.E. Kelly, M.D. Dawson. *Appl. Phys. Lett.*, **105**, 171107 (2014). DOI: 10.1063/1.4900865
- [18] N.I. Solin, S.V. Naumov. *Phys. Solid State*, **45** (3), 486 (2003). DOI: 10.1134/1.1562235.
- [19] M. Buffolo, A. Caria, F. Piva, N. Roccato, C. Casu, C. De Santi, N. Trivellin, G. Meneghesso, E. Zanoni, M. Meneghini. *Phys. Status Solidi A*, **219**, 2100727 (2022). DOI: 10.1002/pssa.202100727
- [20] L. Huang, T. Yu, Z. Chen, Z. Qin, Z. Yang, G. Zhang. *J. Lumin.*, **129** (12), 1981 (2009). DOI: 10.1016/j.jlumin.2009.04.078
- [21] C. Casu, M. Buffolo, A. Caria, C. De Santi, E. Zanoni, G. Meneghesso, M. Meneghini. *Micromachines*, **13** (8), 1266 (2022). DOI: 10.3390/mi13081266
- [22] J. Huang, W. Liu, L. Yi, M. Zhou, D. Zhao, D. Jiang. *Superlattices and Microstruct.*, **113**, 534 (2018). DOI: 10.1016/j.spmi.2017.11.036
- [23] N.A. Tal'nishnikh, A.E. Ivanov, E.I. Shabunina, N.M. Shmidt. *Opt. Spectrosc.*, **131** (11), 1423 (2023). DOI: 10.61011/EOS.2025.04.61414.7296-24.

Translated by D.Safin